

Cytotoxic Potential of Amygdaline Zinc Nano Particles on PC3 and MCF7 Cell Lines

Neihaya H.Zaki¹, Montaha A. Al-Saffar² and Sarah A.Mahmood³

¹Department of Biology, College of Science, Mustansiriyah University, Baghdad, Iraq.

^{2,3}Department of Community Health Techniques, Institute of Medical Technology, Baghdad, Iraq.

Corresponding author email: neihaya1@gmail.com

ABSTRACT

Recently, the development of antitumor drugs has been gradually transformed from cytotoxic drugs to develop new targeted drugs and low toxicity with high specificity drugs. In this study, amygdalin ZnO-Nps were synthesized by adding plant extract and exhibited as white pellet, then characterized by UV-Vis. Spectroscopy which showed an absorption peak at 261 nm, and Scanning Electron Microscope were exhibited size of the nano particle ranged between (20.00–30.26) nm and aggregated as helical shape. While Atomic Force Microscope showed the 2D and 3D of nanoparticles with size of 13.2 nm. The percentage of decreasing viability was increased with increased the concentration, and the IC₅₀ values of the MCF7 and WRL cells were 121.9 and 43.6 µg/mL respectively. Amygdalin ZnO-NPs inhibited proliferation of MCF7 and PC3 cells in a dose-dependent manner. The data demonstrate that amygdalin exerted cytotoxic effect on MCF7 as well as PC3 cells. Treatment with amygdalin induced caspase-9 activation, and induced apoptosis of cancer cells mediated by endogenous mitochondrial pathway, and the significant induction was at 200 µg/ml. In addition, it induced cell membrane permeability, cytochrome- C and total nuclear intensity significantly at 200 µg/ml.

KEY WORDS: AMYGDALINE, ZINC NANO PARTICLES, CYTOTOXIC, CANCER CELL LINES.

INTRODUCTION

Medical plants are used in disease treatment for centuries in many countries, it has the main sources of medicine and drugs due to their compounds and constituents (Bolarinwa, et al 2014), cyanogenic glycosides are normally formed in plants as amygdalin (D-mandelonitrile – β-D -gentiobioside) and there are more than thousands of species in plants, (Boháčová, et al 2019) the mechanism action of cyanogenic glycosides when cell distribution by its action with endogenous enzymes (β-glucosidases and α-hydroxynitrile lyases) (Ge, et al 2007). Many plants products exist that have shown very promising anticancer properties in vitro, such as breast and prostate cancer,

cancer is the major disease-causing death world and due to side effects among chemotherapy, so plant products are used as anticancer, the national cancer institute (NCI) has mentioned about approximately three thousand plant species for cancer therapy and producible anticancer activity (Hwang, et al 2002 and Kang, et al 2000).

Many of researches have illustrated that amygdaline from apricot induce apoptosis (cell death program) by inhibits growing and increasing in number rapidly and interferes with cell cycle progression (Lv et al 2005), as well as amygdalin from apricot causing rapid decrease in mitochondrial membrane, release of cytochrome C and activation of 3, 9 caspase pathways (Savic, et al 2015). Due to treatment of cancer are expensive and severe side effect, so nanoparticles synthesized in biological method are used as anticancer therapeutics, however, there are many plants used in synthesis of zinc nanoparticles for cancer therapy against human cell lines.

Biosc Biotech Res Comm P-ISSN: 0974-6455 E-ISSN: 2321-4007



Identifiers and Pagination

Year: 2021 Vol: 14 No (7) Special Issue

Pages: 235-239

This is an open access article under Creative

Commons License Attribn 4.0 Intl (CC-BY).

DOI: <http://dx.doi.org/10.21786/bbrc/14.7.53>

Article Information

Received: 19th May 2021

Accepted after revision: 20th July 2021

MATERIAL AND METHODS

Apricot seed powder: The apricot seeds were collected from the market, the collected seeds were clean thoroughly under tap water. After washing, the husk was break by a nut cracker, and the raw kernels are subjected to boiling in order to remove the skins of the kernels for 2-4 minutes at 100°C, after that, the boiled kernels are blanched than separated from the rest of the kernels and cut the softer inner material to smaller pieces, then dried by incubation overnight at 37 °C, and then the fully dried seeds were blended in order to obtain a fine powder, which used for extraction purpose (Savic, et al 2012).

Alcohol extraction method for amygdalin from apricot fruit: Dried powder (100g) of apricot seeds was treated with 500 ml of methanol and homogenized for four hours at 37°C, then filtered by using Whatman filter paper, the filtrate solvent was centrifuged at 1500 rpm for 30 min. Then evaporated using rotary evaporator to obtain crude extract and kept until used (Amyrgialaki, et al 2014). **Synthesis of amygdalin ZnO- nanoparticle:** For the synthesis of ZnO-NPs (Habubi, N.F., et al 2018), 1mM stock solutions of Zn acetate (2.1g) was prepared in 100 ml deionized water. The solutions were centrifuged at 6000 rpm for 10 min. to remove bulk impurities, then 100 ml from stock solution in 250 ml Erlenmeyer flasks, and 1g from amygdalin extract was added and stirred gently at temperature of 20, 40, 60 and 80 °C for half hour duration and left 24 hr. at room temperature before being monitored using UV-Vis. Spectrophotometer. Subsequence the solvent of the amygdalin ZnO-NPs liquid sample was evaporated, and the powder was dispersed on to a glass film before analysis by Atomic Force Microscopy (AFM) and Scanning Electron Microscope (SEM).

Characterization of amygdalin ZnO Nanoparticles: **UV-Visible Spectroscopy:** For the first characterization of amygdalin ZnO NPs (CARY, 100CONC plus, UV-Vis– NIR, Split–beam Optics, Dual detectors) was executed in the wavelength range of (200–1100) nm (Freshney, R.I., 2015). **Atomic Force Microscopy (AFM):** AFM was used to record the topography of the amygdalin ZnO-NPs sample. In this mode, the tip of the cantilever dose not contact with the sample surface. The micrograph shows crystalline nature, particle size and roughness of ZnO-NPs. **Scanning Electron Microscope (SEM):** The evaluation of structure, morphology, and elemental composition of ZnO NPs was determined using scanning electron microscopy "SEM, Carl Zeiss Ultra 55".

Cell line culture: Cytotoxicity effect of the extracts in vitro Preparation and maintenance of the cell lines According to (Freshney, 2015), the cancer cell-lines (MCF7 and PC3) were routinely cultured in 25ml flask and incubated under standard conditions (37°C). The medium used for growing of the cells was RPMI-1640, and for cell line maintenance, the flask containing cell suspension was incubated horizontally at 37 °C in the presence of 5% CO₂. **Viable cell counting:** Viable cell counting was performed according to (Ascar, et al 2019)

using the trypan blue exclusion method. Dead cells take up the stain within a few seconds, making them easily distinguished from viable cells. The percent of cell viability was calculated as follows:

$$\text{Cell viability \%} = (\text{No. of unstained cells} / \text{Total No. of cells}) \times 100.$$

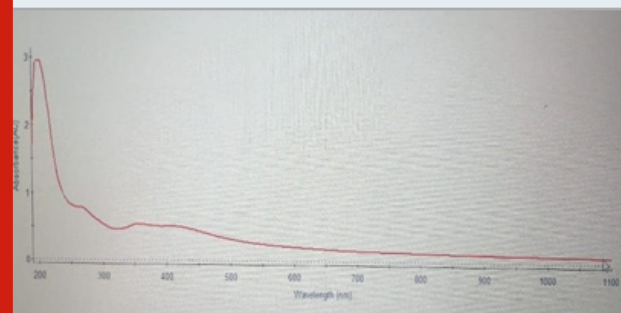
Addition of MTT and cytotoxicity assay: MTT solution (yellow in color) was made by dissolving 5mg MTT crystals in 1ml of PBS solution. After complete solubilization of the dye, the absorbance of the colored solution derived from living cells was read at 570nm with an ELISA reader (Ascar, I.F., et al 2019).

Immunoblot analysis: Immunoblot analysis was performed as described previously by (Lee, and Moon, 2016). Protein extracts in lysis buffer (50 mM Tris, 2% SDS, 1 mM EDTA, 0.1 M DTT, protease inhibitor cocktail) were subjected to immunoblot analysis. Rabbit polyclonal anti-Bax, mouse monoclonal anti-Bcl-2 antibodies, Mouse monoclonal anti-caspase-9 antibody, Rabbit polyclonal anti-PARP, and anti-integrin α 5 antibodies were used in this analysis. The enhanced chemiluminescence system was used for detection. **Statistical Analysis :** The data obtained were subjected to analysis of variance (Dunnett's multiple comparisons test). Results were expressed as mean standard error and values of $p < 0.05$ and < 0.01 , 0.001, were considered significantly. LSD was carried out by SPSS.

RESULTS AND DISCUSSION

Amygdalin ZnO-NPs: A white cluster deposited appeared at the bottom of the flasks indicates the biosynthesis process of amygdalin ZnO-NPs. **UV-Vis. Spectrophotometer:** (Figure 1) showed an absorption peak at 261 nm which indicates the successful biosynthesis of amygdalin ZnO NPs. Researcher of (Ifeanyichukwu, et al 2020) reported that combined vibration of electrons of the biosynthesized nanoparticles indicate with the light wave. And this due to the surface Plasmon resonance (SPR), which is a distinguishing property of the nanoparticles (Thamer, N.A. and AL-Mashhady, L.A., 2016). This result is agreement with result which reported by (17), where absorption peak at 270 nm was obtained.

Figure 1: UV-visible absorption spectrum of amygdalin ZnO NPs synthesized



Scanning Electron Microscope (SEM) Analysis: The SEM analysis was used to observe the physical appearance and the aggregation state of the synthesized ZnO NPs. SEM image showed the dimensions of the particle range between (20.00–30.26) nm and aggregated as helical shape (Figure 2). The morphology of NPs is important sides that participate to the physiochemical properties of the substances (Balogun, et al 2020). A research suggests that the annealing temperature have important effect on the shape of NPs were in some process, the morphology of the NPs seemed to change after calcination at high temperatures (Kuruppu ,et al 2020).

Figure 2: SEM picture of amygdalin ZnO nanoparticles

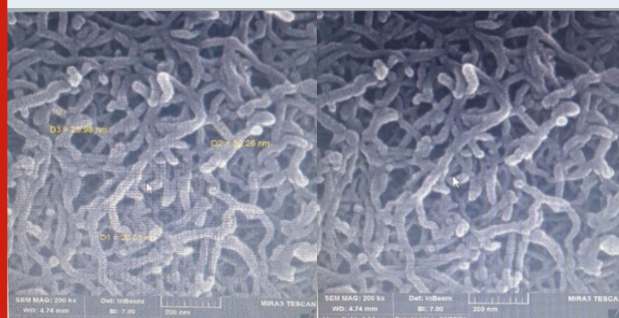


Figure 3: AFM picture of ZnO nanoparticles

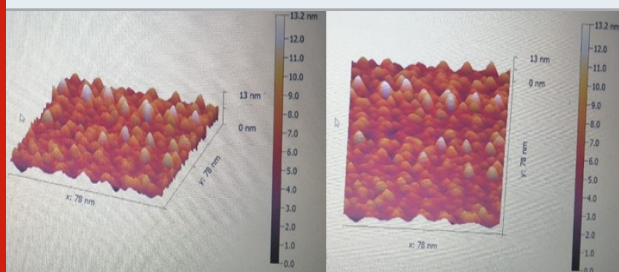


Table 1. Flow cytometric analysis of MCF-7 and WRL68 cells after treated with Amygdalin ZnO-NPs.

Con. of Amygdalin ZnO-NPs	MCF-7		WRL	
	Mean	SD	Mean	SD
400	43.77	5.59	67.63	4.12
200	51.50	1.91	74.04	1.86
100	61.07	2.26	83.64	2.54
50	72.84	1.80	93.52	0.53
25	84.53	2.41	95.02	0.72

AFM analysis: The particle size and roughness of amygdalin ZnO- NPs are found to be increased with the density of it. (Figure 3) showed 2D and 3D AFM images, Hight histogram and section analysis was (78x78 nm) and 13.2 for nanoparticles.

Cytotoxicity effects of amygdaline zinc nano particles: Amygdaline zinc nano particles were used to evaluate their anticancer activity against the breast cancer MCF7

and prostate cancer PC3 cell lines. The cells viability was decreased with increasing the concentration of the ZnO, and the results showed that adding ZnO NPs decrease the cell viability of MCF7 cells, and this decreasing related strongly with the concentrations significantly ($P < 0.05$). The percentage of decreasing viability was (43.7 ± 5.6 , 51.5 ± 1.9 , 61.1 ± 2.6 , 72.8 ± 1.8 and 84.5 ± 2.4) in concentration (400, 200, 100, 50, 25) respectively, while adding the same concentration to the WRL 68 cells did not show significant effect of viability rate ranged between (67.6 ± 4.1 , 74.0 ± 1.8 , 83.6 ± 2.5 , 93.5 ± 0.5 and 95.0 ± 0.7) as shown in table (1), while the IC_{50} values of the MCF7 and WRL cells were 121.9 and 43.6 $\mu\text{g}/\text{mL}$ respectively as shown in figure (4).

Figure 4: Cytotoxicity of AmygdalineZnO NPs with MCF-7 and normal WRL68.

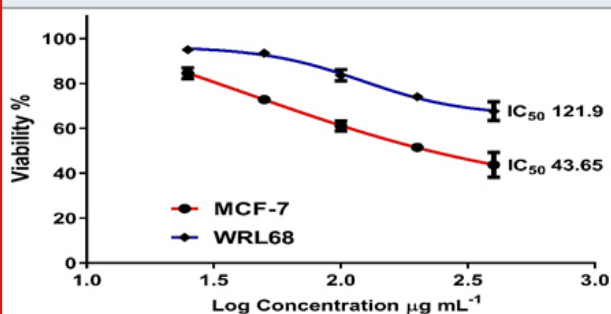
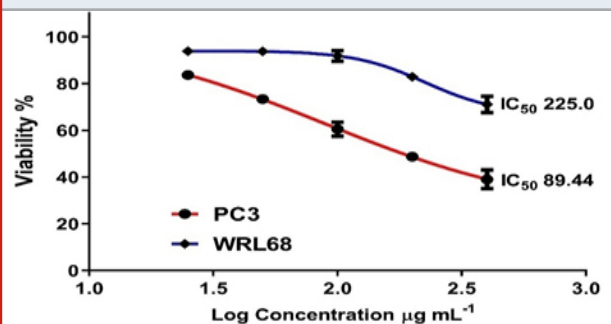


Table 2. Flow cytometric analysis of PC 3 and WRL 68 cells after treated with amygdalin ZnO-NPs.

Con. of Amygdalin ZnO-NPs	PC3		WRL	
	Mean	SD	Mean	SD
400	39.00	4.05	71.10	3.52
200	48.73	0.93	82.91	0.87
100	60.46	2.99	91.82	2.22
50	73.34	0.85	93.79	1.00
25	83.64	0.41	93.87	0.93

Figure 5: Cytotoxicity of amygdalineZnO NPs with PC3 and normal WRL 68.



The results showed that adding amygdaline ZnO NPs decrease the cell viability of PC3 cells, and this decreasing

related strongly with the concentrations significantly ($P < 0.05$). The percentage of decreasing viability was (39.0 ± 4.1 , 48.7 ± 0.9 , 60.5 ± 2.9 , 73.3 ± 0.8 and 83.6 ± 0.4) in concentration (400, 200, 100, 50, 25) respectively, while adding the same concentration to the WRL 68 cells did not show significant effect of viability rate ranged between (71.1 ± 3.5 , 82.9 ± 0.8 , 91.8 ± 2.2 , 93.7 ± 1.0 and 93.8 ± 0.9) as shown in table (2). While the IC_{50} values of the PC3 and WRL cells were 225.0 and 89.44 $\mu\text{g}/\text{mL}$ respectively as shown in figure (5). As shown in Fig.6, amygdalin ZnO-NPs inhibited proliferation of MCF7 and PC3 cells in a dose-dependent manner. The data demonstrate that amygdalin exerted cytotoxic effect on MCF7 as well as PC3 cells.

Figure 6: Amygdalin inhibits cell growth in breast carcinoma cells. The cells were treated with various concentrations of amygdalin for 24 hr

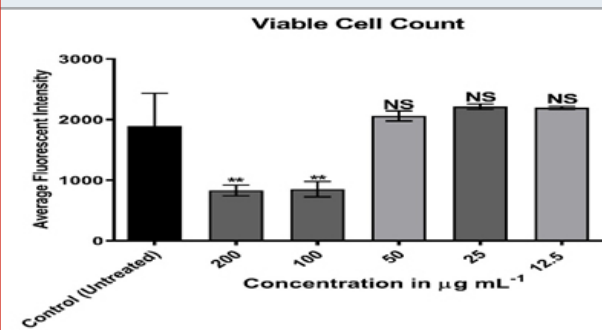
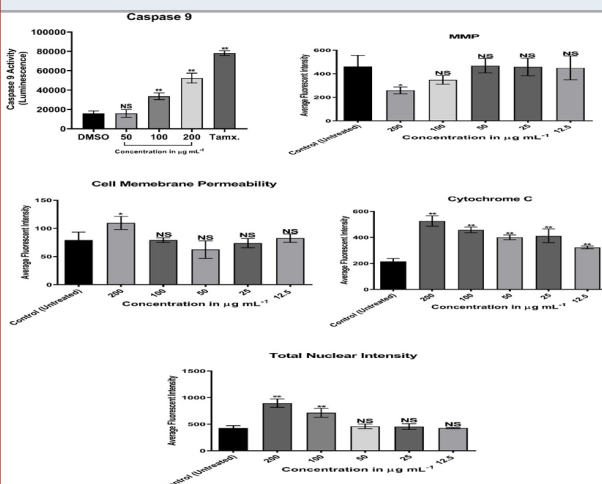


Figure 7: Amygdalin ZnO-NPs regulates apoptosis-related proteins. MCF-7 cells were treated with amygdalin ZnO-NPs at the indicated concentrations (12.5, 25, 50, 100 and 200 $\mu\text{g}/\text{mL}$). The levels of caspase-9, cell membrane permeability, cytochrome C, mitochondrial membrane potential and total nuclear Intensity were determined by immunoblot analysis using specific antibodies.



Researcher of (Reddy and Srividya, 2018) studied the cytotoxicity effect of ZnO NPs against (A549, HEK) human cell lines, and revealed the dose dependent cytotoxicity of zinc oxide nanoparticles using tested cell cultures. The

biosynthesized ZnO NPs due to its semiconducting nature are reported to induce cytotoxicity in cancer cells by the generation of reactive oxygen species on the surface of the particle, the released Zn +2 ions are dissolved in culture media indicating direct interaction of NPs with a membrane of cancer cell resulting in oxidative stress thereby leading to the ultimate death of cancer cells (Jiang, et al 2018).

Amygdalin ZnO-NPs regulates apoptosis-related proteins and signaling molecules: Treatment with amygdalin induced caspase-9 activation in human PC3 prostate cancer cells, and it showed significant activity at concentration of 100 and 200 $\mu\text{g}/\text{ml}$. Amygdalin induced apoptosis of cancer cells mediated by endogenous mitochondrial pathway, and the significant induction was at 200 $\mu\text{g}/\text{ml}$. In addition, it induced cell membrane permeability, cytochrome- C and total nuclear intensity significantly at 200 $\mu\text{g}/\text{ml}$ (Fig. 7).

The MTT viability assay showed that all samples had effects on MCF-7 proliferation in dose and time response manners. With increasing of amygdalin ZnO-NPs concentration and the incubation time, the apoptotic rate was heightened. Compared with the control, there was significant difference ($p < 0.01$). The ingredients of amygdalin activated with β -D-glucosidase had a higher and efficient anticancer activity. It was therefore suggested that this combination strategy may be applicable for treating tumors with a higher activity.

CONCLUSION

Amygdalin is a natural product that owns antitumor activity with less side effects, and ZnO-NPs also have the ability to destroy the cancer cells. Treatment with amygdalin induced caspase-9 activation, and induced apoptosis of cancer cells mediated by endogenous mitochondrial pathway. In addition, it induced cell membrane permeability, cytochrome- C and total nuclear intensity significantly. So, Amygdalin ZnO nanoparticules synthesized by biological method are used as alternative therapeutic against human cell lines

REFERENCES

- Amyrgialaki, E., Makris, D.P., Mauromoustakos, A. and Kefalas, P., 2014. Optimisation of the extraction of pomegranate (*Punica granatum*) husk henolics using water/ethanol solvent systems and response surface methodology. *Industrial Crops and Products*, 59, pp.216-222.
- Ascar, I.F., Al-A'Arabi, S.B. and Alshanon, A.F., 2019. Cytotoxicity and antioxidant effect of ginger gold nanoparticles on thyroid carcinoma cells. *Journal of Pharmaceutical Sciences and Research*, 11(3), pp.1044-1051.
- Bohácová, I., Procházková, S. and Halko, R., 2019. Separation and determination of Amygdalin and unnatural neoAmygdalin in natural food supplements by HPLC-DAD. *Food Additives & Contaminants: Part A*, 36(10), pp.1445-1452.

- Bolarinwa, I.F., Orfila, C. and Morgan, M.R., 2014. Amygdalin content of seeds, kernels and food products commercially-available in the UK. *Food chemistry*, 152, pp.133-139.
- Balogun, S.W., James, O.O., Sanusi, Y.K. and Olayinka, O.H., 2020. Green synthesis and characterization of zinc oxide nanoparticles using bashful (*Mimosa pudica*), leaf extract: a precursor for organic electronics applications. *Sn Applied Sciences*, 2(3), pp.1-8.
- Freshney, R.I., 2015. *Culture of animal cells: a manual of basic technique and specialized applications*. John Wiley & Sons.
- Garikapati, P., Balamurugan, K., Latchoumi, T.P. and Malkapuram, R., 2021. A Cluster-Profile Comparative Study on Machining AlSi 7/63% of SiC Hybrid Composite Using Agglomerative Hierarchical Clustering and K-Means. *Silicon*, 13, pp.961-972.
- Ge, B.Y., Chen, H.X., Han, F.M. and Chen, Y., 2007. Identification of amygdalin and its major metabolites in rat urine by LC-MS/MS. *Journal of Chromatography B*, 857(2), pp.281-286.
- Gopal, V.V. and Kamila, S., 2017. Effect of temperature on the morphology of ZnO nanoparticles: a comparative study. *Applied Nanoscience*, 7(3-4), p.75.
- Habubi, N.F., Abd, A.N., Dawood, M.O. and Reshak, A.H., 2018. Fabrication and Characterization of a p-AgO/PSi/n-Si Heterojunction for Solar Cell Applications. *Silicon*, 10(2), pp.371-376.
- Hwang, E.Y., Lee, J.H., Lee, Y.M. and Hong, S.P., 2002. Reverse-phase HPLC separation of D-amygdalin and neoamygdalin and optimum conditions for inhibition of racemization of amygdalin. *Chemical and pharmaceutical bulletin*, 50(10), pp.1373-1375.
- Ifeanyichukwu, U.L., Fayemi, O.E. and Ateba, C.N., 2020. Green synthesis of zinc oxide nanoparticles from pomegranate (*Punica granatum*) extracts and characterization of their antibacterial activity. *Molecules*, 25(19), p.4521.
- Jiang, J., Pi, J. and Cai, J., 2018. The advancing of zinc oxide nanoparticles for biomedical applications. *Bioinorganic chemistry and applications*, 2018.
- Kang, S.H., Jung, H., Kim, N., Shin, D.H. and Chung, D.S., 2000. Micellar electrokinetic chromatography for the analysis of D-amygdalin and its epimer in apricot kernel. *Journal of Chromatography A*, 866(2), pp.253-259.
- Kuruppu, K.A.S.S., Perera, K.M.K.G., Chamara, A.M.R. and Thiripuranathar, G., 2020. Flower shaped ZnO-NPs; phytofabrication, photocatalytic, fluorescence quenching, and photoluminescence activities. *Nano Express*, 1(2), p.020020.
- Lee, H.M. and Moon, A., 2016. Amygdalin regulates apoptosis and adhesion in Hs578T triple-negative breast cancer cells. *Biomolecules & therapeutics*, 24(1), p.62.
- Lv, W.F., Ding, M.Y. and Zheng, R., 2005. Isolation and quantitation of amygdalin in Apricot-kernel and Prunus Tomentosa Thunb. by HPLC with solid-phase extraction. *Journal of Chromatographic Science*, 43(7), pp.383-387.
- Prasath, S., Validating Data Integrity in Steganographed Images using Embedded Checksum Technique. *International Journal of Computer Applications*, 975, p.8887.
- Reddy, A.R.N. and Srividya, L., 2018. Evaluation of in vitro cytotoxicity of zinc oxide (ZnO) nanoparticles using human cell lines. *J. Toxicol. Risk Assess*, 4(009), p.3.
- Savic, I.M., Nikolic, V.D., Savic-Gajic, I.M., Nikolic, L.B., Ibric, S.R. and Gajic, D.G., 2015. Optimization of technological procedure for amygdalin isolation from plum seeds (*Pruni domesticae* semen). *Frontiers in plant science*, 6, p.276.
- Savic, I.M., Nikolic, V.D., Savic, I.M., Nikolic, L.B. and Stankovic, M.Z., 2012. Development and validation of HPLC method for the determination of amygdalin in the plant extract of plum kernel. *J. Chem. Environ*, 16, pp.80-86.
- Thamer, N.A. and AL-Mashhady, L.A., 2016. Acute toxicity of green synthesis of silver nanoparticles using *Crocus sativus* L. on white albino rats. *Int. J. Phytopharmacol*, 7, pp.13-16.